The Canadian Mineralogist
Vol. 49, pp. 1165-1173 (2011)
DOI: 10.3749/canmin.49.5.1165

ELLINGSENITE, $Na_5Ca_6Si_{18}O_{38}(OH)_{13}•6H_2O$, A NEW MARTINITE-RELATED MINERAL SPECIES FROM PHONOLITE OF THE ARIS ALKALINE COMPLEX, NAMIBIA

VICTOR N. YAKOVENCHUK§, GREGORY YU. IVANYUK, YAKOV A. PAKHOMOVSKY, EKATERINA A. SELIVANOVA AND JULIA A. MIKHAILOVA

Nanomaterials Research Center, Kola Science Center, Russian Academy of Sciences, 14 Fersman Street, Apatity 184209, Russia

SERGEY V. KRIVOVICHEV

St. Petersburg State University, Department of Crystallography, 7–9 Universitetskaya Naberezhnaya, St. Petersburg 199034, Russia, and Nanomaterials Research Center, Kola Science Center, Russian Academy of Sciences, 14 Fersman Street, Apatity 184209, Russia

ANDREY A. ZOLOTAREV

St. Petersburg State University, Department of Crystallography, 7–9 Universitetskaya Naberezhnaya, St. Petersburg 199034, Russia

OLEG A. ZALKIND

Institute of Chemistry and Technology of Rare Elements and Mineral Resources, Kola Science Center, Russian Academy of Sciences, 14 Fersman Street, Apatity 184209, Russia

ABSTRACT

Ellingsenite, $Na_5Ca_6Si_{18}O_{38}(OH)_{13}•6H_2O$, is a new calcium silicate hydrate (CSH) [triclinic, $P\overline{1}$, *a* 9.55(3), *b* 9.395(8), *c* 16.329(3) Å, α 100.2(1), β 94.9(2), γ 117.8(2)°, *V* 1251(8) Å^3, *Z* = 1 (from powder-diffraction data) or *a* 9.576(11), *b* 9.577(11), *c* 16.438(19) Å, α 85.85(2), β 75.23(2), γ 60.142(14)°, *V* 1262(3) Å^3 , *Z* = 1 (from single-crystal diffraction data)], chemically and structurally related to minerals of the gyrolite–reyerite group. The mineral is found in a hydrothermally altered phonolite of the Aris alkaline complex, in Namibia, as snow-white spherules (up to 3 mm in diameter) of well-shaped rhomb-like crystals associated with aegirine, albite, manganoneptunite, microcline, natrolite and polylithionite. The mineral is transparent, colorless in separate crystals, white in aggregates, with a vitreous (separate crystals) to silky (aggregates) luster and a white streak. Cleavage is perfect on {001}, and the fracture is smooth. The Mohs hardness is 4. In transmitted light, the mineral is colorless; dispersion is not observed. Ellingsenite is biaxial (–): α 1.520(2), β 1.534(2), γ 1.536 (589 nm), $2V_{meas}$ 5°. Optical orientation: *X* = **c**. D_{calc} = 2.38 g cm^{-3}, D_{meas} = 2.32(5) g cm^{-3}. The mean chemical composition determined by electron microprobe is: Na_2O 9.26, K_2O 0.23, CaO 17.35, SiO_2 60.35, H_2O 12.5 (Penfield method), for a total of 99.69 wt.%. The empirical formula calculated on the basis of 57 atoms of oxygen is $(Na_{4.95}K_{0.09})_{\Sigma 5.04}(Ca_{5.57}Na_{0.43})_{\Sigma 6.00}Si_{18.10}O_{38}(OH)_{13}•6H_2O$. The simplified formula is $Na_5Ca_6Si_{18}O_{38}(OH)_{13}•6H_2O$. The mineral does not effervesce in 1:1 HCl at room temperature. The strongest X-ray powder-diffraction lines [*d* in Å(I)*hkl*] are: 15.50(100)001, 4.22(16)$\overline{2}$01, 3.159(30)005, 3.023(33)3$\overline{2}$1, 2.791(24)$\overline{2}$14, and 1.827(27)$\overline{5}$11. The crystal-structure model of ellingsenite (R_1 = 0.247) obtained from a crystal of poor quality displays layers of octahedra and tetrahedra of the $T_2O\overline{T}_2$ type with the composition $\{Na_{1.90}Ca_{5.10}[Si_8O_{20}]X_2\}$, where *X* = O, OH, with the interlayer content unresolved. Ellingsenite can be considered as a derivative of martinite, obtained from the latter by intercalation of some additional species (most probably, Na hydrosilicate) in between the adjacent layers of octahedra and tetrahedra. The principal absorption bands in the infrared spectrum include 3460, 1600, 1360 and 1025 cm^{-1} (shoulder at 1140 cm^{-1}) plus four bands in the region of 780–380 cm^{-1}. The mineral is named in honor of Dr. Hans Vidar Ellingsen (born 1930), a well-known Norwegian mineral collector, who found this mineral during his expedition to the Aris complex.

Keywords: ellingsenite, new mineral species, martinite, calcium silicate hydrate, gyrolite group, Aris alkaline complex, Namibia.

§ *E-mail address*: yakovenchuk@ksc.ru

Sommaire

Nous décrivons l'ellingsenite, $Na_5Ca_6Si_{18}O_{38}(OH)_{13}\bullet 6H_2O$, nouveau silicate de calcium hydraté [triclinique, $P\bar{1}$, *a* 9.55(3), *b* 9.395(8), *c* 16.329(3) Å, α 100.2(1), β 94.9(2), γ 117.8(2)°, *V* 1251(8) Å^3, *Z* = 1 (données en diffraction X acquises sur poudre) ou *a* 9.576(11), *b* 9.577(11), *c* 16.438(19) Å, α 85.85(2), β 75.23(2), γ 60.142(14)°, *V* 1262(3) Å^3, *Z* = 1 (données acquises sur monocristal)], qui possède des liens chimiques et structuraux avec les minéraux du groupe de la gyrolite et de la reyerite. L'ellingsenite provient de la phonolite hydrothermalement altérée du complexe alcalin d'Aris, en Namibie. Elle se présente en sphérules blanc-neige atteignant un diamètre de 3 mm, faites de cristaux rhombiques bien formés, associés à aegyrine, albite, manganoneptunite, microcline, natrolite et polylithionite. Le minéral est transparent, incolore en cristaux individuels et blanc en agrégats, avec un éclat vitreux (cristaux individuels) ou soyeux (en agrégats), et une rayure blanche. Le clivage est parfait sur {001}, et la fracture est lisse. La dureté de Mohs est 4. En lumière transmise, le minéral est incolore; aucune dispersion n'est observée. L'ellingsenite est biaxe (–): α 1.520(2), β 1.534(2), γ 1.536 (589 nm), $2V_{mes}$ 5°. L'orientation optique: X = **c**. D_{calc} = 2.38 g cm^{-3}, D_{mes} = 2.32(5) g cm^{-3}. La composition moyenne, établie avec une microsonde électronique, est: Na_2O 9.26, K_2O 0.23, CaO 17.35, SiO_2 60.35, H_2O 12.5 (méthode de Penfield), pour un total de 99.69% (poids). La formule empirique calculée sur une base de 57 atomes d'oxygène est $(Na_{4.95}K_{0.09})_{\Sigma 5.04}(Ca_{5.57}Na_{0.43})_{\Sigma 6.00}Si_{18.10}O_{38}(OH)_{13}\bullet 6H_2O$. La formule simplifiée est $Na_5Ca_6Si_{18}O_{38}(OH)_{13}\bullet 6H_2O$. Le minéral ne montre aucune effervescence dans l'acide HCl 1:1 à température ambiante. Les raies les plus intenses du spectre de diffraction X [*d* en Å(I)*hkl*] sont: 15.50(100)001, 4.22(16)$\bar{2}$01, 3.159(30)005, 3.023(33)3$\bar{2}$1, 2.791(24)$\bar{2}$14, et 1.827(27)$\bar{5}$11. Le modèle structural de l'ellingsenite (R_1 = 0.247), obtenu en utilisant un cristal de piètre qualité, montre des couches d'octaèdres et de tétraèdres de type $T_2O\tilde{T}_2$ ayant une composition $\{Na_{1.90}Ca_{5.10}[Si_8O_{20}]X_2\}$, dans laquelle X = O, OH; les composantes de l'interfeuillet ne sont pas résolues. L'ellingsenite serait un dérivé de la martinite, dérivable de celle-ci par intercalation d'espèces additionnelles (tout probablement hydrosilicate de Na) entre les feuillets adjacents d'octaèdres et de tétraèdres. Parmi les bandes principales d'absorption du spectre infrarouge se trouvent celles à 3460, 1600, 1360 et 1025 cm^{-1} (épaulement à 1140 cm^{-1}) en plus de quatre bandes dans la région 780–380 cm^{-1}. Le nom choisi honore le docteur Hans Vidar Ellingsen (né en 1930), collectionneur norvégien bien connu, qui a découvert ce minéral lors d'une expédition au complexe d'Aris.

(Traduit par la Rédaction)

Mots-clé: ellingsenite, nouvelle espèce minérale, martinite, silicate de calcium hydraté, groupe de la gyrolite, complexe alcalin d'Aris, Namibie.

Introduction

Gyrolite, $Ca_{16}Si_{24}O_{60}(OH)_8\bullet 14H_2O$, is a rare calcium silicate hydrate (CSH) occurring mainly in hydrothermally altered basalts and basaltic tuffs. It is also a common constituent of cement and ceramics, which has led to detailed investigations of gyrolite itself and gyrolite-like minerals and synthetic compounds. Alkali ions can substitute for some of the calcium in the gyrolite structure, and can be intercalated between three-layer Ca–Si–O packets (Baltakys & Siauciunas 2007). In gyrolite from a basalt of Greenland, Na^+ is incorporated into the interlayers if Al^{3+} substitutes for Si^{4+} in the Ca–Si–O layers: $NaCa_{16}AlSi_{23}O_{60}(OH)_8\bullet 14H_2O$ (Merlino 1988). Moreover, if some sodium (about 5 wt.% Na_2O) is present in a reactor vessel, the synthesis of gyrolite accelerates by a factor of two to three times at the same temperature (Baltakys & Siauciunas 2006). Consequently, it was reasonable to expect the presence of Na-rich gyrolite-like phases in alkaline massifs.

Such phases were found first in the Mont Saint-Hilaire massif, Quebec, Canada, as the minerals martinite and lalondeite (McDonald & Chao 2007, 2009) and afterward in hydrothermally altered phonolites of the Aris alkaline complex, Namibia. A gyrolite-like phase from the Aris complex was found in 2002 by amateur Norwegian collectors A. Haugen and H.V. Ellingsen, who suggested a study of their specimens. After being investigated in detail, this gyrolite-like phase has been approved by the Commission on New Minerals and Mineral Names of IMA (IMA 2009–041) as the new mineral species ellingsenite, named after one of the discoverers, Dr. Hans Vidar Ellingsen (born 1930), who has been chairman of the Norwegian Amateur Geological Society and a volunteer at the Geological Museum in Oslo for about 10 years. Type material is deposited at the Mineralogical museum of the St. Petersburg State University, Russia (No. 1/19443), and at the Natural History Museum of the Oslo University, Norway (No. 42188).

Occurrence

Phonolites and other hypabyssal alkaline rocks are widespread in the central part of Namibia (Marsh 1987). The Aris phonolite extrusion is situated about 25 km south of the capital Windhoek (17°13'E, 22°75'S) and has been exploited for breakstone by means of an open cast mine, the Ariskop quarry. This deposit is well known to mineral collectors, who have found here many beautiful specimens of unusual minerals (Wartha *et al.* 2001, Sturla *et al.* 2005).

The ellingsenite-bearing phonolite was found in the Ariskop quarry. It is fine-grained greenish black rock (Fig. 1) consisting mainly of K-feldspar ($K_{0.96–0.98}Na_{0.03–0.04})_{\Sigma 1.00–1.01}[(Al_{0.99–1.02}Si_{2.98–3.00})_{\Sigma 3.99–4.00}O_8]$,

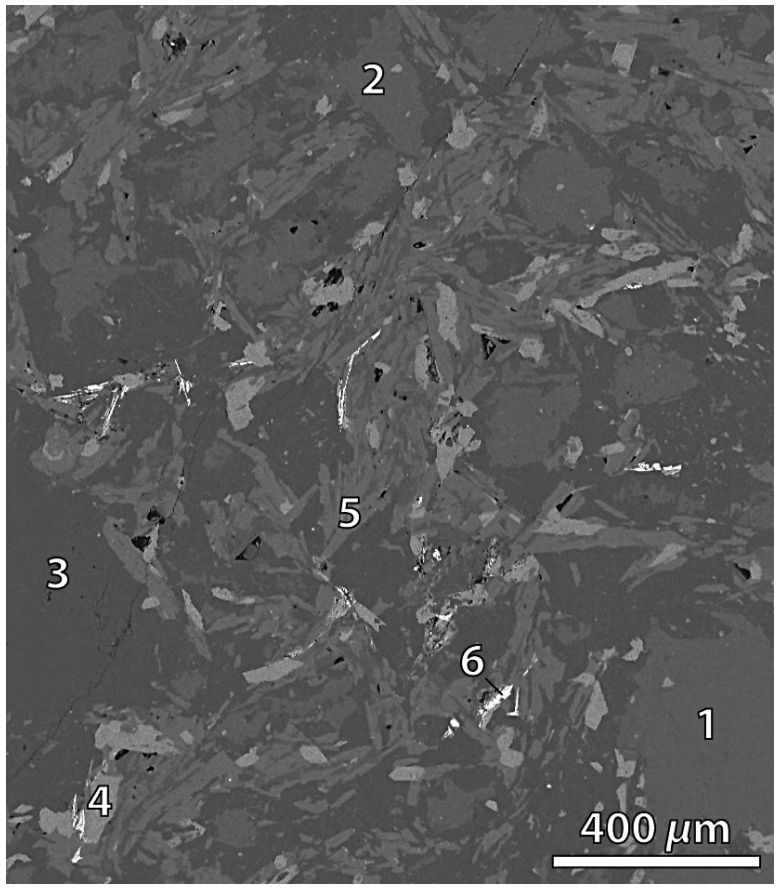

FIG. 1. Phonolite of the Aris extrusion. Domains: 1: nepheline, 2: sodalite, 3: natrolite, 4: aegirine–hedenbergite, 5: K-feldspar, 6: rinkite. Back-scattered electron image.

clinopyroxene of the hedenbergite–aegirine series $(Ca_{0.58–0.15}Na_{0.44–0.89})_{\Sigma 1.02–1.04}(Fe^{3+}_{0.48–0.68}Fe^{2+}_{0.08–0.28}Mg_{0.03–0.16}Mn_{0.04–0.05}Ti_{0.01–0.08}Al_{0.00–0.05})_{\Sigma 0.96–0.98}[(Si_{1.93–2.00}Al_{0.00–0.06}Fe^{3+}_{0.00–0.01})_{\Sigma 2.00}O_6]$, sodalite $(Na_{7.47–7.87}K_{0.01})_{\Sigma 7.48–7.88}[(Si_{5.90–6.07}Al_{6.03–6.05}Fe^{3+}_{0.00–0.06})_{\Sigma 11.95–12.16}O_{24}](Cl_{1.63–1.89}S_{0.00–0.07})_{\Sigma 1.63–1.96}$ and nepheline $K_{0.68}Na_{2.81}[(Si_{4.36}Al_{3.62}Fe^{3+}_{0.07})_{\Sigma 8.05}O_{16}]$. Both sodalite and nepheline are partially replaced by natrolite, $Na_{2.02–2.09}[(Si_{2.97–3.01}Al_{1.99–2.01})_{\Sigma 4.98–5.00}O_{10}]\bullet 2.58–2.98H_2O$. Thorite and rinkite are accessory minerals of this rock.

The phonolite has numerous small roundish cavities or vesicles, up to 3 cm in diameter, coated with crystals of natrolite (predominant), albite and aegirine. The latest mineral assemblage includes manganoneptunite, polylithionite, sazhinite-(Ce), tuperssuatsiaite, tobermorite, villiaumite and ellingsenite, commonly growing on natrolite within the vesicles (Fig. 2). Ellingsenite occurs as separate snow-white spherulites (up to 3 mm in diameter) of well-shaped rhomb-like crystals. Usually, such spherulites have no inclusions; rarely they contain segregations of minute (a few micrometers) roundish grains of an unknown carbonate–silicate of the rare-earth elements.

MORPHOLOGY, PHYSICAL AND OPTICAL PROPERTIES

Ellingsenite forms rhomb-like crystals, flattened on [001] and elongate on [100], with dominant pinacoidal {001} and {*hk*0} forms. Faces {*hk*0} are invariably rounded, and sharp corners are fractally foliated. Usually, the crystals are arranged in sheaf-like and radiating aggregates. No twinning was observed. Cleavage is perfect on (001). The mineral is sectile and has smooth fracture. The hardness is about 4. The density determined by the float–sink method in methylene iodide is 2.32(5) g cm^{-3}. This value is in

good agreement with the calculated density of 2.383 g cm^{-3} (cell from powder data), and 2.363 g cm^{-3} (cell from single-crystal data).

Macroscopically, ellingsenite is colorless (separate crystals) to white (aggregates), and has a vitreous (separate crystals) to silky (aggregates) luster. The mineral is transparent, with a white streak. It is biaxial negative, with indices of refraction α 1.520(2), β 1.534(2), γ 1.536 (589 nm), $2V_{meas}$ 5°. Optical orientation: X = **c**. In transmitted light, the mineral is colorless, without dispersion. A Gladstone–Dale calculation provides a compatibility index of 0.003, which is regarded as superior (Mandarino 1981).

Chemical Composition

The chemical composition of ellingsenite has been studied by wavelength-dispersion spectrometry using a Cameca MS–46 electron microprobe (Geological Institute, Kola Science Centre, Russian Academy of Sciences, Apatity) operating at 20 kV, 20–30 nA and 10 μm beam diameter. The following standards were used: lorenzenite (Na, Ti), diopside (Si, Ca) and wadeite (K). The content of H_2O was determined by the Penfield method on purified material. The absence of carbon and fluorine was confirmed by energy-dispersive spectrometry using a Röntec spectrometer coupled with a LEO 1450 scanning electron microscope. Table 1 provides mean analytical results for two spherulites of ellingsenite (two analyses per spherulite).

The empirical formula, based on 57 atoms of oxygen, is $(Na_{4.95}K_{0.09})_{\Sigma 5.04}(Ca_{5.57}Na_{0.43})_{\Sigma 6.00}Si_{18.10}O_{38}(OH)_{13.00}\bullet 6H_2O$. Without respect to crystal-structure refinement, the simplified formula of ellingsenite is $Na_5Ca_6Si_{18}O_{38}(OH)_{13}\bullet 6H_2O$ (Z = 1).

The mineral is insoluble in 1:1 HCl at room temperature.

The Crystal-Structure Model

Experimental

Several platy crystals of ellingsenite selected for data collection were examined on a STOE Image Plate Diffraction System II (IPDS II) and Bruker APEX CCD diffractometers. In most cases, diffraction spots were diffuse, and indexing was problematic. However, two reasonably good crystals have been measured on Bruker APEX CCD diffractometer operated at 50 kV and 40 mA. More than a hemisphere of three-dimensional data were collected for each crystal using monochromatic Mo$K\alpha$ X-radiation, with frame widths of 0.5° in ω, and with a 90 s count for each frame. Diffraction data of the same crystals have also been collected using the STOE IPDS II diffractometer in order to inspect their diffraction patterns. In both cases, the (001) sections of reciprocal space contained round and sharp diffraction spots (Fig. 3a). However, the (100) section and, especially, the (010) section indicated that most of the reflections are either split or accompanied by diffuse streaks, which indicated a highly imperfect quality of the crystals (Figs. 3b, c). Below, we report on the data

TABLE 1. CHEMICAL COMPOSITION OF ELLINGSENITE

Constituent	Mean	Range	SD
Na_2O wt.%	9.26	9.02 – 9.51	0.20
SiO_2	60.35	59.30 – 61.43	0.90
K_2O	0.23	0.18 – 0.25	0.03
CaO	17.35	17.09 – 17.54	0.19
H_2O	12.5		
Total	99.69		

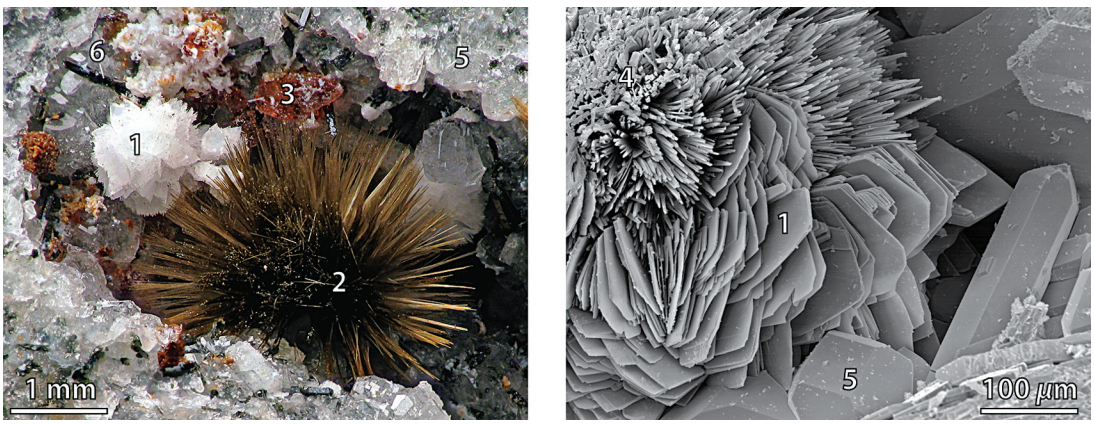

FIG. 2. Ellingsenite (1), tuperssuatsiaite (2), villiaumite (3), tobermorite (4), natrolite (5) and aegirine (6) in a vesicle within phonolite.

obtained for the crystal of better quality. The unit-cell parameters (Table 2) were refined using least-squares techniques. The intensity data were integrated and corrected for Lorentz, polarization, and background effects using the Bruker AXS suite of programs. The partial structure-model was obtained in space group $P\bar{1}$ by direct methods, which allowed us to locate some cation and anion positions of the layers of octahedra and tetrahedra (see below). Our attempts to locate interlayer sites were unsuccessful, as were attempts to refine displacement parameters of atoms in anisotropic approximation. These problems were undoubtedly a consequence of the poor diffraction-quality of the ellingsenite crystals. We have also tried to refine the structure model in the $P1$ space group but without any improvement in the structure parameters. The partial model included all atomic positional parameters, isotropic-displacement parameters for all atoms, and a refinable weighting scheme of the structure factors. The final refinement resulted in $R_1 = 0.247$ for 3553 unique observed reflections. The final atomic coordinates and anisotropic-displacement parameters are given in Table 3, and selected bond-lengths are given in Table 4. The list of observed and calculated structure-factors have been submitted to the Depository of Unpublished Data on the MAC website [document Ellingsenite CM49_1165].

TABLE 2. ELLINGSENITE: CRYSTALLOGRAPHIC DATA AND REFINEMENT PARAMETERS FOR THE PARTIAL MODEL OF THE STRUCTURE

a (Å)	9.576(11)	α (°)	85.85(2)
b (Å)	9.577(11)	β (°)	75.23(2)
c (Å)	16.438(19)	γ (°)	60.142(14)
V (Å^3)	1262(3)		
Space group	$P\bar{1}$	Z	1
Crystal size (mm)	0.12 × 0.12 × 0.01		
Radiation	Mo*K*α	2θ range (°)	2.56–56.38
Total reflections	13949	R_1	0.2466
Unique reflections	6121	wR_2	0.5264
Unique $\|F_o\| \geq 4\sigma_F$	3553	*S*	1.089

TABLE 3. COORDINATES, ISOTROPIC DISPLACEMENT PARAMETERS (Å^2), AND SITE-OCCUPANCY FACTORS (SOF) OF ATOMS IN THE PARTIAL MODEL OF THE STRUCTURE OF ELLINGSENITE

Atom	*x*	*y*	*z*	U_{iso}	SOF
Na1	1/2	0	1/2	0.021(4)	Na
Na2	0.8448(13)	-0.2128(13)	-0.7107(6)	0.017(3)	$Na_{0.86(4)}$
Ca1	0.3564(6)	-0.2907(6)	-0.5025(3)	0.0152(10)	Ca
Ca2	0.0818(5)	-0.8582(5)	-0.5130(2)	0.0125(9)	Ca
Ca3	0.7756(8)	-0.4159(7)	-0.4942(3)	0.018(2)	$Ca_{0.55(6)}Na_{0.45(6)}$
Si1	0.4595(8)	-0.4440(8)	-0.2301(4)	0.0166(13)	Si
Si2	0.8056(8)	-0.6630(7)	-0.3328(3)	0.0125(12)	Si
Si3	0.2987(8)	0.4577(8)	-0.3268(4)	0.0139(12)	Si
Si4	0.0501(7)	-0.0324(7)	-0.3309(3)	0.0114(12)	Si
Si5	0.9247(8)	-0.4153(8)	-0.3246(4)	0.0147(12)	Si
Si6	0.4183(8)	-0.1603(7)	-0.3312(3)	0.0128(12)	Si
Si7	0.5453(8)	0.0888(7)	-0.3254(3)	0.0135(12)	Si
Si8	0.7899(8)	-0.1100(8)	-0.2225(4)	0.0161(13)	Si
O1	0.085(2)	-0.0778(19)	-0.4272(9)	0.015(3)	O
O2	0.930(3)	-0.365(3)	-0.4182(12)	0.033(4)	O
O3	0.664(2)	0.067(2)	-0.4171(9)	0.019(3)	O
O4	0.370(2)	0.479(2)	-0.4222(10)	0.021(3)	O
O5	0.815(2)	-0.6616(19)	-0.4293(9)	0.015(3)	O
O6	0.7816(19)	-0.1980(18)	-0.5624(9)	0.013(3)	O
O7	0.392(2)	0.271(2)	-0.3022(10)	0.021(3)	O
O8	0.757(3)	-0.091(3)	-0.1237(13)	0.042(5)	O
O9	0.870(2)	-0.550(2)	-0.3030(10)	0.021(3)	O
O10	0.932(2)	-0.841(2)	-0.3092(9)	0.018(3)	O
O11	0.638(2)	0.044(2)	-0.2506(9)	0.018(3)	O
O12	0.109(2)	0.496(2)	-0.3075(10)	0.021(3)	O
O13	0.495(2)	-0.231(2)	-0.4249(9)	0.017(3)	O
O14	0.308(2)	-0.438(2)	-0.2593(10)	0.019(3)	O
O15	0.963(2)	-0.121(2)	-0.2697(10)	0.020(3)	O
O16	0.625(2)	-0.606(2)	-0.2730(10)	0.023(4)	O
O17	0.454(2)	-0.018(2)	-0.3154(9)	0.018(3)	O
O18	0.214(2)	-0.072(2)	-0.3035(10)	0.019(3)	O
O19	0.482(2)	-0.291(2)	-0.2622(10)	0.020(3)	O
O20	0.802(2)	-0.272(2)	-0.2505(10)	0.023(4)	O
O21	0.421(3)	-0.440(3)	-0.1317(13)	0.041(5)	O
O22	0.385(13)	0.084(13)	-0.187(6)	0.050*	$H_2O_{0.25(5)}$
O23	0.915(5)	-0.222(4)	-0.857(2)	0.050*	$H_2O_{0.73(5)}$

TABLE 4. SELECTED BOND-LENGTHS (Å) IN THE PARTIAL MODEL OF THE STRUCTURE OF ELLINGSENITE

Na1–O6	2.387(15)	2×	Si2–O5	1.566(15)	
Na1–O13	2.469(16)	2×	Si2–O16	1.591(18)	
Na1–O3	2.638(16)	2×	Si2–O10	1.614(17)	
Na1–O17	2.958(15)	2×	Si2–O9	1.640(18)	
<Na1–O>	2.61		<Si2–O>	1.60	
Na2–O23	2.32(3)		Si3–O4	1.586(17)	
Na2–O6	2.35(2)		Si3–O14	1.591(17)	
Na2–O18	2.51(2)		Si3–O12	1.607(19)	
Na2–O12	2.53(2)		Si3–O7	1.627(18)	
Na2–O10	2.54(2)		<Si3–O>	1.60	
Na2–O17	2.54(2)				
Na2–O7	2.54(2)		Si4–O1	1.579(15)	
Na2–O9	2.59(2)		Si4–O18	1.599(18)	
Na2–O22	2.84(10)		Si4–O15	1.606(18)	
<Na2–O>	2.53		Si4–O10	1.611(17)	
			<Si4–O>	1.60	
Ca1–O13	2.330(16)				
Ca1–O4	2.367(18)		Si5–O2	1.57(2)	
Ca1–O3	2.384(17)		Si5–O9	1.605(18)	
Ca1–O1	2.426(16)		Si5–O20	1.627(18)	
Ca1–O5	2.429(16)		Si5–O12	1.629(19)	
Ca1–O4	2.452(18)		<Si5–O>	1.61	
<Ca1–O>	2.4				
			Si6–O13	1.565(16)	
Ca2–O6	2.271(15)		Si6–O19	1.616(17)	
Ca2–O3	2.303(17)		Si6–O17	1.618(17)	
Ca2–O2	2.31(2)		Si6–O18	1.643(18)	
Ca2–O5	2.402(16)		<Si6–O>	1.61	
Ca2–O1	2.401(16)				
Ca2–O1	2.437(16)		Si7–O3	1.595(16)	
<Ca2–O>	2.35		Si7–O11	1.611(16)	
			Si7–O7	1.615(18)	
Ca3–O6	2.315(16)		Si7–O17	1.616(18)	
Ca3–O13	2.379(17)		<Si7–O>	1.61	
Ca3–O2	2.39(2)				
Ca3–O5	2.405(17)		Si8–O8	1.58(2)	
Ca3–O4	2.475(18)		Si8–O15	1.593(18)	
Ca3–O2	2.63(2)		Si8–O20	1.597(19)	
<Ca3–O>	2.43		Si8–O11	1.615(17)	
			<Si8–O>	1.60	
Si1–O21	1.56(2)				
Si1–O16	1.599(19)				
Si1–O14	1.613(18)				
Si1–O19	1.619(18)				
<Si1–O>	1.60				

Results

The crystal structure of ellingsenite is similar to the structures of other members of the reyerite–gyrolite group (Merlino 1988, Bonaccorsi & Merlino 2005, McDonald & Chao 2007, 2009). It contains layers of octahedra and tetrahedra of the $T_2O\overline{T}_2$ type, where O is a sheet of octahedra of brucite type, and T_2 and $\overline{T}_2$ are $[Si_4O_{10}]$ sheets of tetrahedra with six tetrahedra pointing their non-shared vertices toward the O sheet and two tetrahedra pointing their non-shared vertices in the opposite direction (Figs. 4a, b). The $T_2O\overline{T}_2$ layer in ellingsenite has the composition $\{Na_{1.90}Ca_{5.10}[Si_8O_{20}]X_2\}$, where X represents O, OH. The O layer is composed from Na1, Ca1, Ca2, and Ca3 cations octahedrally coordinated by six anions each [there are two long Na1–O bonds of 2.958(15) Å in the coordination environment of the Na site that make its total coordination number equal to 8]. The only interlayer position that could be located from our data is the Na2 site, with the total occupancy 0.86(4) based on the site-scattering function of Na. This site is [9]-coordinated with seven anions belonging to the $T_2O\overline{T}_2$ layer and the other two being low-occupancy anion sites that are tentatively assigned to the H_2O molecules (Fig. 5).

X-Ray Powder-Diffraction Pattern

The powder X-ray-diffraction pattern of purified ellingsenite was obtained by means of the URS–1 instrument operated at 40 kV and 30 mA with a 114.7 mm Debye–Scherrer camera and Fe$K\alpha$ radiation (Table 5). Unit-cell parameters determined from powder patterns are a 9.55(3), b 9.395(8), c 16.329(3) Å, α 100.2(1), β 94.9(2)°, γ 117.8(2)° and V 1251(8) Å^3 (Z = 1).

Infrared Spectroscopy

The infrared-absorption spectrum of purified ellingsenite was recorded using a Specord M–80 spectrometer at the Institute of Chemistry and Technology of Rare

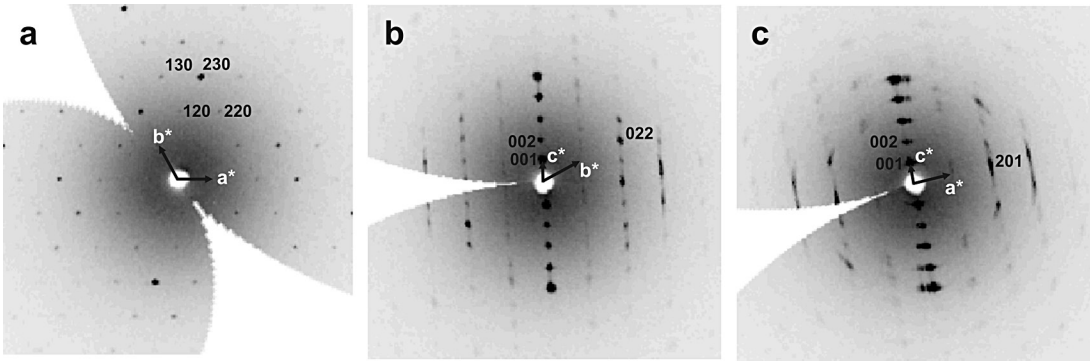

FIG. 3. Reconstructed (001) (a), (100) (b), and (010) (c) sections of diffraction space for the crystal of ellingsenite.

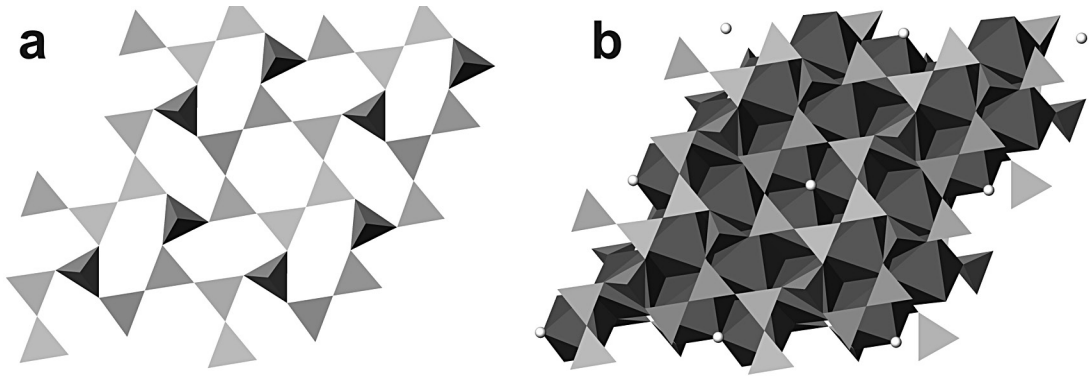

FIG. 4. Sheet of $T2$ (a) and top view of the $T2O2$ layer (b) in the structure of ellingsenite (white circles show the Na2 positions).

Elements and Mineral Resourses (Kola Science Center, Russian Academy of Sciences). The spectrum (Fig. 6) has absorption bands at 380, 480, 600, 780, 880, 1025, 1095, 1140, 1360, 1600, 3260, 3460 and 3600 cm^{-1} and is similar to the IR spectrum of gyrolite (Baltakys & Siauciunas 2007) and lalondeite (McDonald & Chao 2009). Wide bands at 3460 and 1630 cm^{-1} are caused by vibrations of molecules of H_2O in the interlayers. A band of medium strength at 1360 cm^{-1} corresponds to the products of dissociation of silanol groups, whereas two high-frequency shoulders of this band as well as the band of medium strength at 3260 cm^{-1} are due to Si–(OH) vibrations. Bands at 3600 and 780 cm^{-1} can be assigned as corresponding to vibrations of OH groups in stretching and libration modes, respectively.

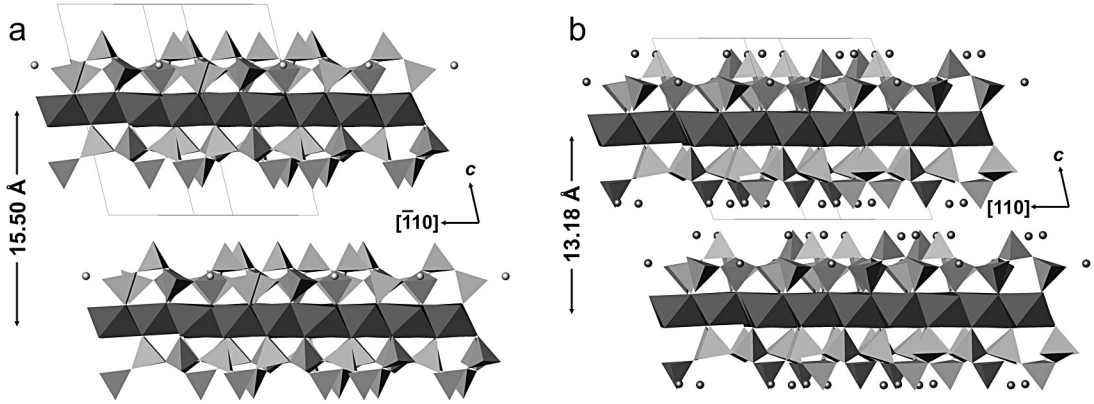

FIG. 5. Crystal structures of ellingsenite (a) and martinite (b) projected parallel to the extension of the *T2O2* layers. Circles indicate positions of Na^+ ions and H_2O molecules. Note that the interlayer space in ellingsenite is ~ 2.3 Å thicker than that in martinite.

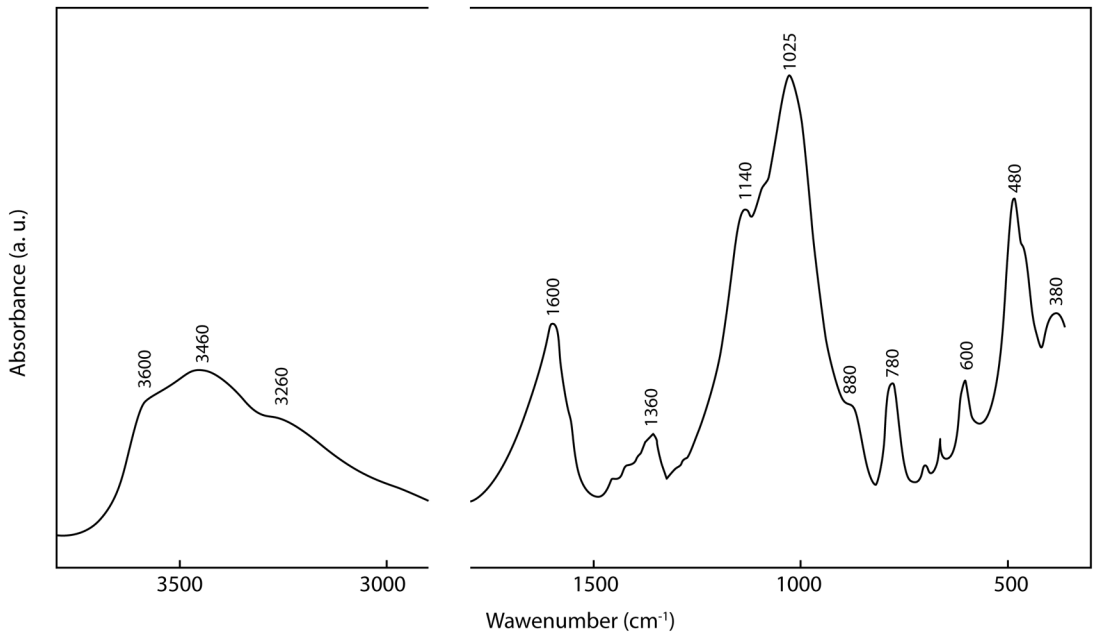

FIG. 6. Infrared spectrum of ellingsenite.

Discussion

Our refinement of the crystal structure, the infrared spectra and an investigation of the physical properties of ellingsenite show that it is a mineral clearly related with the reyerite–gyrolite group of minerals (Bonaccorsi & Merlino 2005, McDonald & Chao 2007, 2009). Consequently, the structural formula of ellingsenite should be rewritten on the basis of the $[Si_8O_{20}]$ radical: $(Na_{1.84}K_{0.04})_{\Sigma 1.88}(Ca_{2.46}Na_{0.54})_{\Sigma 3.00}[Si_8O_{19.34}(OH)_{0.66}]\bullet 5.34H_2O$ or, simplifying, $Na_2(Ca,Na)_3[Si_8O_{19}(O,OH)]\bullet 5H_2O$ ($Z = 2$). However, the calculated density will be unreliably low (2.09 g cm^{-3}) in this case and the Gladstone–Dale compatibility index will be unreliably high (0.168). For this reason, we suppose that a part of the silica is located within the "muddy" Na–H_2O interlayers, according to the appropriate formula $NaCa_3[Si_8O_{19}(OH)]\bullet\{(NaOH)_{1.5}Si(OH)_4(H_2O)_3\}$ ($Z = 2$).

According to the nomenclature of the reyerite–gyrolite group of minerals (Bonaccorsi & Merlino 2005, McDonald & Chao 2007, 2009), the structure can be described using the structural scheme $T_2O\bar{T}_2XT_2O\bar{T}_2$, where X is the interlayer content. Among the minerals of the group, the same structural scheme is possessed by martinite, $(Na,\square,Ca)_{12}Ca_4(Si,S,B)_{14}B_2O_{38}(OH,Cl)_2F_2\bullet 4H_2O$ (McDonald & Chao 2007). Table 6 provides a comparison of the structural and physical parameters of ellingsenite and martinite, whereas Figure 5 shows projections of their structures parallel to the extension of the $T_2O\bar{T}_2$ layers. One sees that the spacing between the adjacent $T_2O\bar{T}_2$ layers in ellingsenite is about 2.3 Å larger than that in martinite, which makes our suggestion about possible incorporation of Na silicate units into the interlayer in ellingsenite quite reasonable. However, we point out that a more detailed investigation of ellingsenite structure is needed in order to test this hypothesis, which can only be possible after crystals of better quality are found. In general, it seems possible to characterize ellingsenite as martinite with some additional species (*e.g.*, Na hydrosilicate) intercalated in between the adjacent layers of octahedra and tetrahedra.

The layered structure of ellingsenite makes it interesting from the material science point of view. Miyake *et al.* (1990) synthesized Al-substituted gyrolite $Ca_8Si_{11.32}Al_{0.68}Na_{0.44}O_{30}(OH)_4\bullet 6.6H_2O$ and found it to be a cation-exchanger for K^+ and Cs^+. El-Korashy (2004) established that Al-substituted gyrolite may be used to remove heavy metals from wastewaters. Also, gyrolite can be exploited for the removal of DNA impurities from solutions containing supercoiled plasmid (Winters *et al.* 2003) and for making pillared materials (Ferraris & Gula 2005). We believe that ellingsenite can be more effective than either gyrolite or lalondeite for all these purposes owing to its higher Na content in comparison with gyrolite and lower density in comparison with lalondeite.

Experiments by hydrothermal synthesis showed that the temperature interval 175–200°C is optimal for the crystallization of Na-containing gyrolite, but is not sufficient to form Na-free gyrolite (Baltakys & Siauciunas 2007). On the other hand, an increase in both temperature and Na content initiates the transformation of gyrolite into pectolite, whereas high pH (>9.5) and the presence of Al stabilizes gyrolite and prevents this transformation (Baltakys & Siauciunas 2006, Bankauskaite & Baltakys 2009). Therefore, we can conclude that ellingsenite is a low-temperature hydrothermal mineral,

TABLE 5. X-RAY POWDER-DIFFRACTION DATA FOR ELLINGSENITE

I	d_{obs}	d_{calc}	*h*	*k*	*l*	*I*	d_{obs}	d_{calc}	*h*	*k*	*l*
100	**15.50**	**15.7698**	0	0	1	5	2.6370	2.6365	3	$\bar{2}$	3
4	8.31	8.2911	1	0	0	3	2.5430	2.5425	$\bar{2}$	$\bar{1}$	5
5	7.89	7.8849	0	0	2	5	2.4130	2.4160	$\bar{1}$	3	3
		7.8810	1	$\bar{1}$	1	5	2.3120	2.3351	0	1	6
8	6.48	6.4887	0	$\bar{1}$	2	5	2.2880	2.2992	$\bar{2}$	$\bar{1}$	6
13	5.20	5.2566	0	0	3	2	2.1580	2.1517	1	3	1
14	**4.98**	**5.0485**	0	1	2	5	2.0550	2.0506	$\bar{2}$	3	5
14	**4.89**	**4.8879**	$\bar{1}$	$\bar{1}$	1	7	1.9410	1.9385	$\bar{2}$	$\bar{3}$	2
3	4.67	4.6524	$\bar{2}$	1	1	**27**	**1.8270**	**1.8295**	$\bar{5}$	1	1
16	**4.22**	**4.2139**	$\bar{2}$	0	1			1.8285	$\bar{1}$	$\bar{4}$	2
12	3.82	3.8182	1	$\bar{2}$	3			1.8259	$\bar{5}$	1	2
8	3.67	3.6681	$\bar{2}$	1	3	2	1.7160	1.7129	$\bar{2}$	$\bar{1}$	9
6	3.39	3.4008	2	$\bar{1}$	3	3	1.6540	1.6539	$\bar{1}$	4	5
30	**3.1590**	**3.1540**	0	0	5	2	1.5780	1.5785	$\bar{2}$	0	10
33	**3.0230**	**3.0221**	3	$\bar{2}$	1	3	1.5590	1.5585	$\bar{1}$	5	3
24	**2.7910**	**2.7922**	$\bar{2}$	$\bar{1}$	4	3	1.5310	1.5348	1	$\bar{3}$	10

TABLE 6. COMPARISON OF ELLINGSENITE AND MARTINITE

Mineral	Ellingsenite	Martinite[§]
Formula	$Na_8Ca_6Si_{18}O_{38}(OH)_{13}\bullet 6H_2O$	$(Na,\square,Ca)_{12}Ca_4(Si,S,B)_{14}B_2O_{38}(OH,Cl)_2F_2\bullet 4H_2O$
Crystal system	Triclinic	Triclinic
Space group	$P\bar{1}$	$P\bar{1}$
a (Å)	9.576(11)	9.5437(7)
b (Å)	9.577(11)	9.5349(6)
c (Å)	16.438(19)	14.0268(10)
α (°)	85.85(2)	108.943(1)
β (°)	75.23(2)	74.154(1)
γ (°)	60.142(14)	119.780(1)
V Å^3	1262(3)	1038.1(1)
Z	1	1
Strongest lines in powder X-ray pattern *d* in Å (*I*)	15.50(100) 4.22(16) 3.159(30) 3.023(33) 2.791(24) 1.827(27)	13.18(100) 6.58(43) 2.968(37) 3.29(34) 2.908(27) 3.02(17)
Density (g•cm^{-3})	2.32	2.51
Mohs hardness	4	4
Color	Colorless	Colorless
Optical character	Biaxial (–)	Biaxial (–)
α	1.520	1.529
β	1.534	1.549
γ	1.536	1.551
2*V* (°)	5	35
Orientation	*X* = **c**	*X* = **c**
Crystal habit	Spherules of rhomb-like crystals	Triangular or roughly hexagonal plates
Cleavage	Perfect on {001}	Perfect on {001}

[§] McDonald & Chao (2007).

which crystallized from a residual alkaline solution in vacuoles at temperatures about 160–180°C. We believe these conditions to be optimal for the synthesis of ellingsenite as well.

Acknowledgements

We thank A. Haugen for fruitful cooperation and P.A. Williams for critical discussion of the results obtained. We are grateful to Robert F. Martin, Frédéric Hatert and Igor V. Pekov for many constructive comments on the manuscript and editorial help. S.V.K. and A.A.Z. were supported in this work by the Russian Federal Grant-in-Aid Program (state contract #16.518.11.7096).

References

Baltakys, K. & Siauciunas, R. (2006): The influence of γ-Al_2O_3 and Na_2O on the formation of gyrolite in the stirring suspension. *J. Mater. Sci.* **41**, 4799-4805.

Baltakys, K. & Siauciunas, R. (2007): Formation of gyrolite in the CaO–quartz–Na_2O–H_2O system. *Mater. Sci.-Poland* **25**, 1089-1100.

Bankauskaite, A. & Baltakys, K. (2009): The sorption of copper ions by gyrolite in alkaline solution. *Mater. Sci.-Poland* **27**, 899-908.

Bonaccorsi, E. & Merlino, S. (2005): Modular microporous minerals: cancrinite–davyne group and C–S–H phases. *In* Micro- and Mesoporous Mineral Phases (G. Ferraris & S. Merlino, eds.). *Rev. Mineral. Geochem.* **57**, 241-290.

El-Korashy, S.A. (2004): Cation exchange of alkali metal hydroxides with some hydrothermally synthesized calcium silicate compounds. *J. Ion Exch.* **15**, 2-9.

Ferraris, G. & Gula, A. (2005): Polysomatic aspects of microporous minerals – heterophyllosilicates, palysepioles and rhodesite-related structures. *In* Micro- and Mesoporous Mineral Phases (G. Ferraris & S. Merlino, eds.). *Rev. Mineral. Geochem.* **57**, 69-104.

Mandarino, J.A. (1981): The Gladstone–Dale relationship. IV. The compatibility concept and its application. *Can. Mineral.* **19**, 441-450.

Marsh, J.S. (1987): Evolution of a strongly differentiated suite of phonolites from the Klinghardt Mountains, Namibia. *Lithos* **20**, 41-58.

McDonald, A.M. & Chao, G.Y. (2007): Martinite, a new hydrated sodium calcium fluorborosilicate species from Mont Saint-Hilaire, Quebec: description, structure determination and genetic implications. *Can. Mineral.* **45**, 1281-1292.

McDonald, A.M. & Chao, G.Y. (2009): Lalondeite, a new hydrated sodium–calcium fluorsilicate species from Mont Saint-Hilaire, Quebec: description and crystal structure. *Can. Mineral.* **47**, 181-191.

Merlino, S. (1988): Gyrolite: its crystal structure and crystal chemistry. *Mineral. Mag.* **52**, 377-387.

Miyake, M., Iwaya, M. & Suzuki, T. (1990): Aluminum-substituted gyrolite as cation exchanger. *J. Am. Ceram. Soc.* **73**, 3524-3527.

Sheldrick, G.M. (1997): SHELXL97. *Program for the Refinement of Crystals Structures*. University of Göttingen, Göttingen, Germany.

Sturla, M., Yakovenchuk, V.N. & Bonacina, E. (2005) Aris, Namibia: geo-paragenesi e minerali. *MICRO (localitatà)* **2005**, 55-80.

Wartha, R., Palfi, A.G., Niedermayer, G., Brandstätter, F. & Petersen, O. (2001): Der Aris-Phonolith-Komplex und seine Mineralien. Namibia. *Zauberwelt edler Steine und Kristalle* (S. Jahn, O. Medenbach, G. Niedermayr, G. Schneider, eds.). Bode Verlag GmbH, Haltern, Germany (172-179).

Winters, M.A., Richter, J.D., Sagar, S.L., Lee, A.L. & Lander, R.J. (2003): Plasmid DNA purification by selective calcium silicate adsorption of closely related impurities. *Biotechnol. Progr.* **19**, 440-447.

Received September 7, 2010, revised manuscript accepted October 17, 2011.